

## Localization of Binding Sites for Epidermal Growth Factor (EGF) in Rat Kidney: Evidence for the Existence of Low Affinity EGF Binding Sites on the Brush Border Membrane

Dong Chool Kim,<sup>1</sup> Manabu Hanano,<sup>1</sup> Yasushi Kanai,<sup>2</sup> Norio Ohnuma,<sup>2</sup> and Yuichi Sugiyama<sup>1,3</sup>

Received November 21, 1991; accepted April 8, 1992

We investigated the renal distribution of <sup>125</sup>I-EGF in the filtering perfused rat kidney using an acid washing technique. Trichloroacetic acid-precipitable <sup>125</sup>I-EGF radioactivity was eluted from both the renal vein and the urinary cannulae, the former regarded as representing the antiluminal, and the latter the luminal, cell surface bound <sup>125</sup>I-radioactivity. The addition of excess unlabeled EGF (20 nM) to the perfusate completely inhibited the binding of <sup>125</sup>I-EGF to the antiluminal membrane but did not inhibit that of <sup>125</sup>I-EGF to the luminal membrane. On the other hand, the order of relative density of <sup>125</sup>I-EGF binding sites in the *in vivo* kidney determined by autoradiography was cortex > inner medulla > outer medulla. After the i.v. administration of excess unlabeled EGF together with <sup>125</sup>I-EGF, the renal uptake of <sup>125</sup>I-EGF was inhibited completely in the inner medulla, but only by 50% in the cortex and outer medulla, suggesting the presence of nonsaturable luminal uptake of EGF in the cortex and outer medulla. After i.v. administration of <sup>125</sup>I-EGF, a change in position of silver grains from the luminal cell surface membrane to the intracellular space was observed in the proximal convoluted tubules. In conclusion, in addition to the previously identified uptake mechanism of circulating EGF through high-affinity binding sites on the antiluminal cell surface membrane, the reabsorption mechanism of filtered EGF through low-affinity binding sites on the luminal cell surface membrane was demonstrated. *In vivo* autoradiography showed the gradual internalization of EGF from the luminal cell surface membrane to the intracellular space of the proximal convoluted tubule.

**KEY WORDS:** receptor-mediated endocytosis; acid wash; internalization; filtering kidney; epidermal growth factor (EGF); nonsaturable uptake of EGF from the luminal side of the kidney, luminal uptake of EGF in the proximal convoluted tubules.

### INTRODUCTION

The binding of EGF to its receptor on the cell surface membrane induces various physiological effects (1,2). Hirata and Orth (3) measured the EGF concentration in various human fluids and showed that milk and urine contain a high concentration of EGF. Although EGF eliminated in the urine was isolated and its primary structure was determined (4), the origin of urinary EGF has not been clarified. The kidney

was found to be abundant in EGF mRNA (5). EGF has been immunolocalized to the luminal cell surface membrane (separating the luminal fluid from the cell cytoplasm) lining the thick ascending limb of Henle (TALH) and the distal convoluted tubule (DCT) (6). It is likely that the presence of EGF immunoreactivity in the mouse kidney is the result of EGF synthesis rather than filtration of serum EGF (6). Therefore, it is plausible that the prepro-EGF localized to the luminal cell surface membranes of the TALH and DCT is cleaved to release EGF into the urine (6). However, there is no evidence so far that there are EGF receptors on the luminal cell surface membranes along the nephron. On the other hand, the application of EGF to the antiluminal side (the side of the basement membrane, upon which the epithelial layer rests, separating the cytoplasm from the interstitial fluid) induced physiological effects on isolated nephron segments (2,7-9).

We have demonstrated that the relative contributions of the liver and kidney to the early phase distribution clearance of plasma EGF after its i.v. bolus administration were 70 and 13%, respectively (10). When EGF was infused intravenously at a constant rate, the plasma EGF concentration reached steady state 90 min after the start of infusion, and the contributions of the liver and kidney to the total elimination clearance in the steady state were 70 and 17%, respectively (11-13). The kidney is thus the second most important organ in the removal of circulating plasma EGF, compared to the liver. Subsequently, we investigated the relative contributions of antiluminal and luminal EGF uptake in the perfused rat kidney (filtering and nonfiltering kidney), and it was demonstrated that receptor-mediated endocytosis of EGF through the antiluminal membrane plays an important role in the renal uptake of EGF (14,15). The purpose of the present study is to investigate the binding and uptake of EGF via the luminal membrane and to identify the binding sites of EGF on the luminal membrane morphologically.

### MATERIALS AND METHODS

#### Materials

Biosynthetic human epidermal growth factor (EGF), obtained from *Escherichia coli* via the synthesized coding sequence described previously (16), was used in all experiments. Sodium iodide-125 (100 mCi/ml) was purchased from the Radiochemical Center (Amersham Corp., Arlington Heights, IL). The EGF was radiolabeled with <sup>125</sup>I-Na by the chloramine-T method (17). Unreacted <sup>125</sup>I-Na was removed by a Sephadex G-25 column, and the <sup>125</sup>I-EGF was eluted in the void volume. The <sup>125</sup>I-EGF had a specific activity of 0.5 to 1.0 mCi/nmol. <sup>14</sup>C-Inulin (2.6 μCi/mg) was purchased from ICN Radiochemicals (Division of ICN Biomedicals, Irvine, CA), and its purity as determined by gel filtration (Sephadex G-25) was more than 98%. Bovine serum albumin (fraction V) was purchased from Sigma, and all other chemicals were obtained from commercial sources and were of analytical grade.

#### Isolated Perfused Rat Kidney

The isolated perfused rat kidney technique previously

<sup>1</sup> Faculty of Pharmaceutical Sciences, University of Tokyo, Hongo, Bunkyo-ku, Tokyo 113, Japan.

<sup>2</sup> Clinical Pharmacology and Bio. Pharm. Center of Suntory Co., 2716-1 Chioda, Ohra, Gunma 370-05, Japan.

<sup>3</sup> To whom correspondence should be addressed.

described by our laboratory (18) has been slightly modified. After male Wistar rats weighing 300–380 g were anesthetized with ether, the renal right artery was cannulated via the mesenteric artery without interruption of blood flow. The renal vein and the ureter were also cannulated. The perfusate composition is as follows: Krebs-Hensleit buffer (NaCl, 116 mM; KCl, 4 mM; CaCl<sub>2</sub>, 2 mM; KH<sub>2</sub>PO<sub>4</sub>, 1.5 mM; MgSO<sub>4</sub>, 2.4 mM; NaHCO<sub>3</sub>, 25 mM) containing fraction V bovine serum albumin, glucose (1 mg/ml), <sup>14</sup>C-inulin, and a mixture of amino acids (*l*-methionine, 0.5 mM; *l*-alanine, 2 mM; glycine, 2 mM; *l*-serine, 2 mM; *l*-proline, 2 mM; *l*-isoleucine, 1 mM; *l*-aspartic acid, 3 mM; *l*-arginine, 1 mM; *l*-cystine, 0.5 mM; *l*-glutamate, 0.5 mM) (19,20). Monoiodotyrosine (1 mM) was included in perfusate containing <sup>125</sup>I-EGF to inhibit deiodination of degradation products (21). Immediately after the operation on the right kidney, the kidney was excised and then perfused in a closed-circuit system. Unless otherwise noted, kidneys were perfused at 37°C with 100 ml of perfusate in a recirculatory mode. The pH 7.4 perfusate was continuously gassed with a mixture of 95% O<sub>2</sub>–5% CO<sub>2</sub>. When kidneys were studied in the filtering mode, the perfusate albumin concentration was 5 g/dl, and the effective perfusion pressure was approximately 100 mmHg.

#### Determination of Cell Surface Bound EGF by an Acid Washing Technique

The kidneys were perfused in the filtering mode. After a 10-min stabilization period, the perfusate was switched to a perfusate containing EGF. After a 20-min recirculatory perfusion of <sup>125</sup>I-EGF only or together with 20 nM unlabeled EGF in the filtering kidney, the perfusate containing <sup>125</sup>I-EGF was switched to EGF-free perfusate and the filtering kidney was washed out for 6 min to remove any <sup>125</sup>I-EGF remaining in the antiluminal extracellular and luminal spaces and the perfusion medium was then switched to a pH 4.0 acid buffer (NaCl, 58 mM; KCl, 4 mM; CaCl<sub>2</sub>, 2 mM; KH<sub>2</sub>PO<sub>4</sub>, 1.5 mM; MgSO<sub>4</sub>, 2.4 mM; NaHCO<sub>3</sub>, 25 mM; CH<sub>3</sub>COOH, 58 mM) and washed for an additional 6 min to release the <sup>125</sup>I-EGF molecules bound to the basolateral membrane and brush border membrane. During the washing process, the outflows from the renal vein and urinary canulae were collected at 1-min intervals and the trichloroacetic acid (TCA)-precipitable <sup>125</sup>I radioactivities in the outflows were determined. The total released <sup>125</sup>I-EGF radioactivity detected in the venous outflow has been considered to be <sup>125</sup>I-EGF that was bound to the antiluminal membrane. The <sup>125</sup>I radioactivity remaining in the kidney after the acid washing was treated as the internalized <sup>125</sup>I-EGF. The results were normalized by the amount of EGF added to the perfusate.

#### *In Vivo* Uptake Study

A tracer amount of <sup>125</sup>I-EGF or <sup>125</sup>I-EGF plus excess unlabeled EGF (17 nmol) was administered together with <sup>14</sup>C-inulin (1.5 μmol) through the femoral vein to male Wistar rats anesthetized with ether. At designated times, the blood was withdrawn through the femoral artery cannula, and 10 min after the administration of drugs, the kidney was perfused with 50 ml of 0.9% NaCl solution (10 ml/min/rat) and excised. The plasma was obtained from blood by cen-

trifugation and the TCA-precipitable <sup>125</sup>I radioactivity in the plasma was determined. The kidney, perfused with 0.9% NaCl solution, was dissected into cortex, outer medulla, and inner medulla. The sections were assayed for <sup>125</sup>I radioactivity in a gamma counter (Model ARC-300, Aloka Co., Ltd., Tokyo) with a counting efficiency of 80%. The sections (0.1 mg) were dissolved in 10 ml aquasol at 37°C overnight. The radioactivities for <sup>14</sup>C in dissolved sections were determined in a Tri-Carb liquid scintillation spectrometer (Packard Instruments Model 3255, Downers Grove, IL). The appropriate crossover correction was used to separate the radioactivities, <sup>14</sup>C and <sup>125</sup>I. The apparent uptake clearance (CL<sub>up,app</sub>) of <sup>125</sup>I-EGF in each renal fraction was calculated by dividing the <sup>125</sup>I radioactivity in each fraction by the AUC<sub>(0–10)</sub>, which is the area under the plasma concentration–time curve of <sup>125</sup>I-EGF from time 0 to 10 min.

#### Autoradiographic Study (*in Vivo*)

A tracer amount of <sup>125</sup>I-EGF (10 μCi) alone was administered through the femoral vein to male Wistar Rats (230–260 g body wt) anesthetized with ether. At different time intervals (2 and 10 min), the kidneys were perfused through the heart with 50 ml of NaCl (0.9%) and subsequently perfused with 50 ml of 2% glutaraldehyde in saline solution. Immediately, the kidney was excised, and the <sup>125</sup>I-radioactivity was measured in a gamma counter. The separated kidney was preserved overnight in 2% glutaraldehyde, dehydrated by means of a serial treatment of ethanol solutions from 50 to 100%, and finally, preserved in 100% xylene until dissection. The paraffin sections (20 μm thick) prepared from the dehydrated kidney were mounted on glass slides and dried. The X-ray films (IX-150, Fuji Film, Tokyo) were tightly apposed to the sections, exposed for 60 days at 4°C, and developed for the quantitative measurement of density (22). The densities of enlarged autoradiographic images were measured in an image analyzer (IBAS, Carl Zeiss, Germany) that converted the amount of light into grey values. The tissue radioactivity was estimated using standards for autoradiography.

To observe the binding sites of <sup>125</sup>I-EGF at the microscopic level, three paraffin sections (4 μm thick) were mounted on glass slides and dipped into nuclear track emulsion (NTB-2, Eastman Kodak) and exposed for 60 days. After the preparations were developed and fixed, they were stained with hematoxylin–eosin, and the observed silver grains were counted with the use of image analyzer. The variances in grain density among the sections were less than 5%.

## RESULTS

#### Release of <sup>125</sup>I-EGF into the Venous Outflow and Urinary Cannula by Acid Washing in the Isolated Perfused Rat Kidney

Twenty minutes after the recirculatory perfusion of <sup>125</sup>I-EGF only (or together with excess unlabeled EGF), the cell surface bound <sup>125</sup>I-EGF was separated from the internalized <sup>125</sup>I-EGF using an acid washing technique (Fig. 1). These results are also summarized in Table I. <sup>125</sup>I radioactivity levels appearing in the outflows from renal vein and urinary

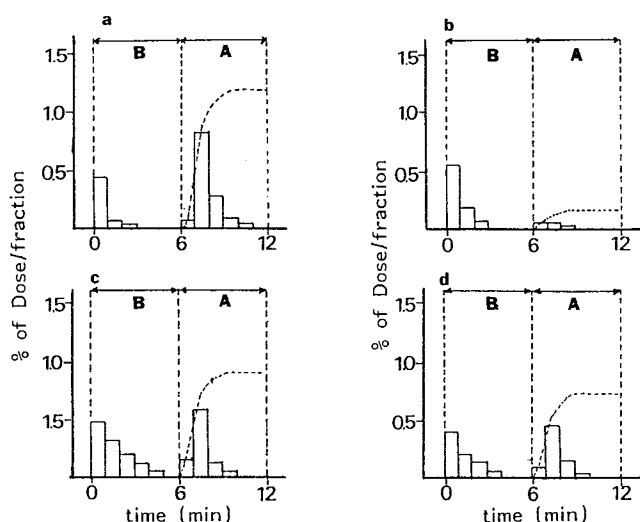


Fig. 1. Acid-washing method to determine separately the  $^{125}\text{I}$ -EGF bound to antiluminal and luminal cell surface and the internalized  $^{125}\text{I}$  EGF. Open bars represent the  $^{125}\text{I}$  radioactivity elution pattern in the outflows during the washing procedure. B and A represent the buffer and acid washing periods, respectively. Dashed lines represent the time course of cumulative TCA-precipitable  $^{125}\text{I}$  radioactivity during the acid washing period. (a,b) Outflows from the renal vein cannula; (c,d) outflows from the urinary cannula; (a,c) the tracer  $^{125}\text{I}$ -EGF perfusion experiment; (b,d) the tracer  $^{125}\text{I}$ -EGF plus 20 nM unlabeled EGF perfusion experiment. The results were normalized by the amount of EGF added to the perfusate. See details under Materials and Methods.

cannulae approached zero 6 min after changing the perfusate to normal buffer free of  $^{125}\text{I}$ -EGF, showing that the extracellular space on the antiluminal side and the luminal space were almost completely washed. When the normal buffer was changed to acid buffer, the  $^{125}\text{I}$  radioactivity in the outflows from renal vein and urinary cannulae again began to appear. The accumulated  $^{125}\text{I}$  radioactivities in the renal vein and urinary outflows after acid washing were considered to represent the amounts of antiluminal and luminal cell surface bound  $^{125}\text{I}$ -EGF, respectively. In addition, the  $^{125}\text{I}$  radioac-

Table I. Parameters for EGF Handling by Filtering Rat Kidney<sup>a</sup>

	Tracer $^{125}\text{I}$ EGF	Tracer $^{125}\text{I}$ EGF plus 20 nM EGF
$\text{LR}_s(\text{ALM})/\text{L}$ (ml/kidney) <sup>b</sup>	$2.47 \pm 0.10$	$0.202 \pm 0.064$
$\text{LR}_s(\text{LM})/\text{L}$ (ml/kidney) <sup>b</sup>	$1.01 \pm 0.34$	$0.717 \pm 0.441$
$\text{LR}_i/\text{L}$ (ml/kidney) <sup>c</sup>	$8.60 \pm 2.17$	$1.76 \pm 0.22$

<sup>a</sup> After the recirculatory perfusion of EGF, the amounts of cell surface bound and internalized EGF were determined by the acid washing technique. Under the experimental conditions, the concentration of EGF was kept essentially constant for 20 min.

<sup>b</sup>  $\text{LR}_s(\text{ALM})$  and  $\text{LR}_s(\text{LM})$  represent the amounts of cell surface bound EGF on the antiluminal and luminal membranes, respectively. L is the perfusate concentration of EGF. The values of  $\text{LR}_s(\text{ALM})/\text{L}$  were reported previously (15).

<sup>c</sup>  $\text{LR}_i$  is the amount of internalized EGF at 20 min.

Table II. Time Profile of the Optical Density of  $^{125}\text{I}$ -EGF<sup>a</sup>

Time (min)	$X_r$ [optical density/area]		
	COR	OM	IM
2 ( $n = 3$ )	$0.642 \pm 0.091$	$0.270 \pm 0.132$	$0.305 \pm 0.120$
10 ( $n = 2$ )	0.571	0.164	0.318

<sup>a</sup> After the i.v. administration of tracer  $^{125}\text{I}$ -EGF (10  $\mu\text{Ci}/\text{rat}$ ), the kidney was fixed by perfusion with 2% glutaraldehyde solution. The paraffin sections (20  $\mu\text{m}$  in thickness) prepared from the dehydrated kidney were mounted on glass slides and the X-ray films were apposed tightly to the sections, exposed, and developed for the quantitative measurement of density. The densities of enlarged autoradiographic images were measured with an image analyzer (IBAS, Carl Zeiss, Germany). COR, cortex; OM, outer medulla; IM, inner medulla. See details in the text.

tivity remaining in the kidney after the acid washing can be regarded as internalized  $^{125}\text{I}$ -EGF. The antiluminal cell surface bound and internalized  $^{125}\text{I}$ -EGF decreased to  $1/12$  and  $1/5$ , respectively, in the presence of excess unlabeled EGF (20 nM) in the perfusate, but the luminal cell surface bound  $^{125}\text{I}$ -EGF did not (Table I).

#### Localization of $^{125}\text{I}$ -EGF Binding Sites *In Vivo*

Two and ten minutes after i.v. administration of  $^{125}\text{I}$ -EGF (10  $\mu\text{Ci}/\text{rat}$ ), the intrarenal distribution of  $^{125}\text{I}$  radioactivity was determined by autoradiography. The distribution of optical density of  $^{125}\text{I}$ -EGF was cortex > inner medulla ~ outer medulla at 2 min and cortex > inner medulla > outer medulla at 10 min after the administration (Table II, Fig. 2). However, these results should be interpreted carefully since

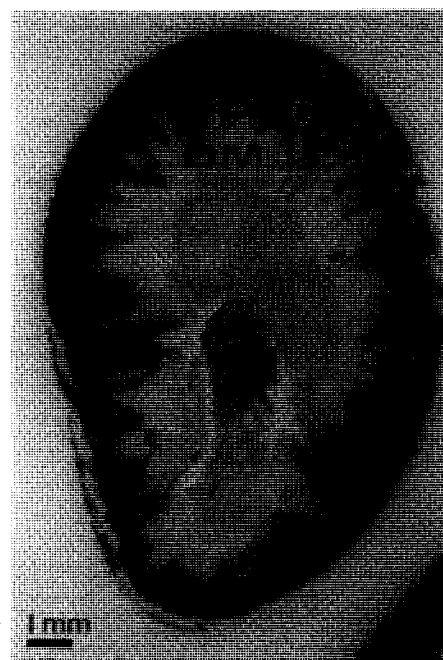


Fig. 2. Intrarenal distribution of  $^{125}\text{I}$  radioactivity 10 min after i.v. administration of  $^{125}\text{I}$ -EGF (10  $\mu\text{Ci}/\text{rat}$ ) determined using X-ray film autoradiography. COR, cortex; OM, outer medulla; IM, inner medulla.

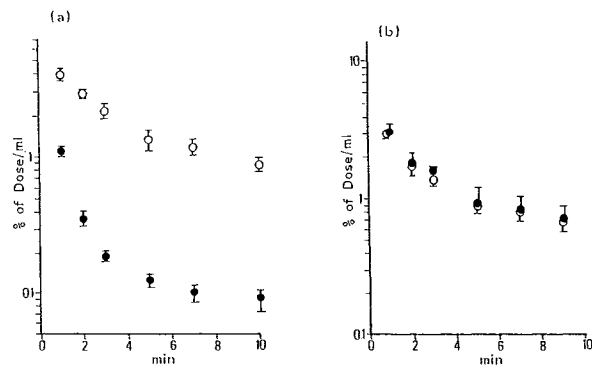


Fig. 3. The time profiles of plasma concentration after the i.v. administration of  $^{125}\text{I}$ -EGF plus  $^{14}\text{C}$ -inulin (filled circles) or  $^{125}\text{I}$ -EGF plus  $^{14}\text{C}$ -inulin together with 17 nmol unlabeled EGF (open circles). (a)  $^{125}\text{I}$ -EGF time profiles; (b)  $^{14}\text{C}$ -inulin time profiles. See details under Materials and Methods.

it is possible that the tissue-associated radioactivity may have come partly from degraded products.

Figure 3 illustrates the time profiles of TCA-precipitable  $^{125}\text{I}$  radioactivity ( $^{125}\text{I}$ -EGF) and  $^{14}\text{C}$ -inulin in the plasma after the i.v. bolus administration of  $^{125}\text{I}$ -EGF plus  $^{14}\text{C}$ -inulin or  $^{125}\text{I}$ -EGF plus  $^{14}\text{C}$ -inulin together with excess unlabeled EGF (17 nmol). The elimination of plasma  $^{125}\text{I}$ -EGF was remarkably delayed after the coadministration of excess unlabeled EGF (Fig. 3a), but that of plasma  $^{14}\text{C}$ -inulin was not (Fig. 3b). The intrarenal distribution of  $^{125}\text{I}$  and  $^{14}\text{C}$  radioactivities 10 min after the i.v. administration is shown in Table III. To wash out the  $^{125}\text{I}$  and  $^{14}\text{C}$  radioactivities remaining in the lumen and extracellular space, we perfused the kidney with 50 ml of saline before excision. The extracellular marker substance ( $^{14}\text{C}$ -inulin) was used to assess the nonspecific distribution of  $^{125}\text{I}$ -EGF since  $^{14}\text{C}$ -inulin has almost the same molecular weight ( $\sim 5000$ ) as  $^{125}\text{I}$ -EGF (MW  $\sim 6000$ ). Therefore the  $^{14}\text{C}$  radioactivity remaining in the kidney after the saline perfusion can estimate the contribution of nonspecific  $^{125}\text{I}$ -EGF distribution to the total  $^{125}\text{I}$ -EGF radioactivity remaining in the kidney. Table III summarizes

the  $\text{CL}_{\text{up}}$  values of  $^{125}\text{I}$ -EGF in each kidney fraction, which are corrected by the corresponding  $\text{CL}_{\text{up,app}}$  of  $^{14}\text{C}$ -inulin. The  $\text{CL}_{\text{up}}$  value of  $^{125}\text{I}$ -EGF of the cortex and outer medulla decreased to approximately 50% and that of the inner medulla to 5% with the coadministration of 17 nmol unlabeled EGF as compared with the tracer  $^{125}\text{I}$ -EGF experiment (Table III).

We also investigated the intrarenal distribution of  $^{125}\text{I}$  radioactivity morphologically using autoradiography after i.v. bolus administration of tracer  $^{125}\text{I}$ -EGF (Fig. 4). The silver grains were observed in the proximal convoluted tubules (PCT; S1), proximal tubules (PT; S2 + S3) other than PCT, glomeruli, and cortical collecting duct (CCD) and were broadly distributed over the whole outer medulla. Also, the thin limb of Henle (TLH) and collecting duct (CD) in the inner medulla were abundant in silver grains. Table IV summarizes the results of grain counting. Concerning the outer medulla, we did not count grains in different regions because of difficulty in both identifying the renal tubules morphologically and counting the low grain density. The grain density on the luminal cell surface membrane of cortical PCT was three times larger than that in the intracellular space at 2 min after the i.v. administration of  $^{125}\text{I}$ -EGF, but the relation between the luminal membrane and the intracellular space concerning grain density was reversed at 10 min after  $^{125}\text{I}$ -EGF administration, which shows the movement of radioactivity from the luminal cell surface membrane to the intracellular space. On the other hand, the grain density ratio of antiluminal membrane to the intracellular space of the PT (S2 + S3) was 7 at 2 min and decreased to 2 at 10 min after the i.v. administration of  $^{125}\text{I}$ -EGF (Table IV), suggesting the movement of radioactivity from the antiluminal to the intracellular space.

## DISCUSSION

EGF receptors have been identified in cultured mesangial cells (7), PT (2), CCD (9), and inner medullary collecting duct (IMCD) (23). Until the present, these receptors have been identified only on the antiluminal side of renal tubules

Table III. The Apparent Uptake Clearance of  $^{125}\text{I}$ -EGF in the Rat Kidney<sup>a</sup>

	$\text{AUC}_{(0-10)}$ (dose min/ml) <sup>b</sup>		Tissue <sup>c</sup>	$X_t$ (% dose/g) <sup>d</sup>		$\text{CL}_{\text{up,app}}$ (ml/min/g) <sup>e</sup>		$\text{CL}_{\text{up}}$ (ml/min/g) <sup>f</sup>	
	A	B		A	B	A	B	A	B
$^{125}\text{I}$ -EGF	4.04 ± 0.49	19.7 ± 2.3	COR	6.22 ± 0.86	16.3 ± 0.9	1.58 ± 0.29	0.84 ± 0.09	1.49 ± 0.34	0.75 ± 0.04
			OM	3.84 ± 0.36	9.42 ± 1.30	0.96 ± 0.10	0.47 ± 0.06	0.79 ± 0.09	0.42 ± 0.03
			IM	2.96 ± 0.34	1.65 ± 0.29	0.58 ± 0.14	0.08 ± 0.01	0.72 ± 0.12	0.04 ± 0.01
$^{14}\text{C}$ -Inulin	15.3 ± 1.3	14.2 ± 0.8	COR	1.65 ± 0.99	1.17 ± 0.32	0.10 ± 0.05	0.08 ± 0.03		
			OM	1.00 ± 0.34	0.69 ± 0.13	0.06 ± 0.02	0.05 ± 0.01		
			IM	0.61 ± 0.27	0.84 ± 0.35	0.04 ± 0.02	0.06 ± 0.02		

<sup>a</sup> Tracer amount of  $^{125}\text{I}$ -EGF (3  $\mu\text{Ci}/\text{rat}$ ) only (A) or  $^{125}\text{I}$ -EGF plus 17 nmol unlabeled EGF (B) was i.v. injected into the rat together with  $^{14}\text{C}$ -inulin.

<sup>b</sup>  $\text{AUC}_{(0-10)}$  is the area under the plasma concentration-time profile of each compound from time 0 to 10 min. The plasma concentrations were normalized by dose.

<sup>c</sup> COR, cortex; OM, outer medulla; IM, inner medulla.

<sup>d</sup>  $X_t$  is the dose-normalized accumulated radioactivity of each compound per gram of each kidney fraction.

<sup>e</sup>  $\text{CL}_{\text{up,app}}$  is the apparent uptake clearance, which is calculated by dividing the  $X_t$  value by  $\text{AUC}_{(0-10)}$ .

<sup>f</sup>  $\text{CL}_{\text{up}}$  is the corrected uptake clearance, which is calculated by subtracting the  $\text{CL}_{\text{up,app}}$  of  $^{125}\text{I}$ -EGF with that of  $^{14}\text{C}$ -inulin in the same rat.

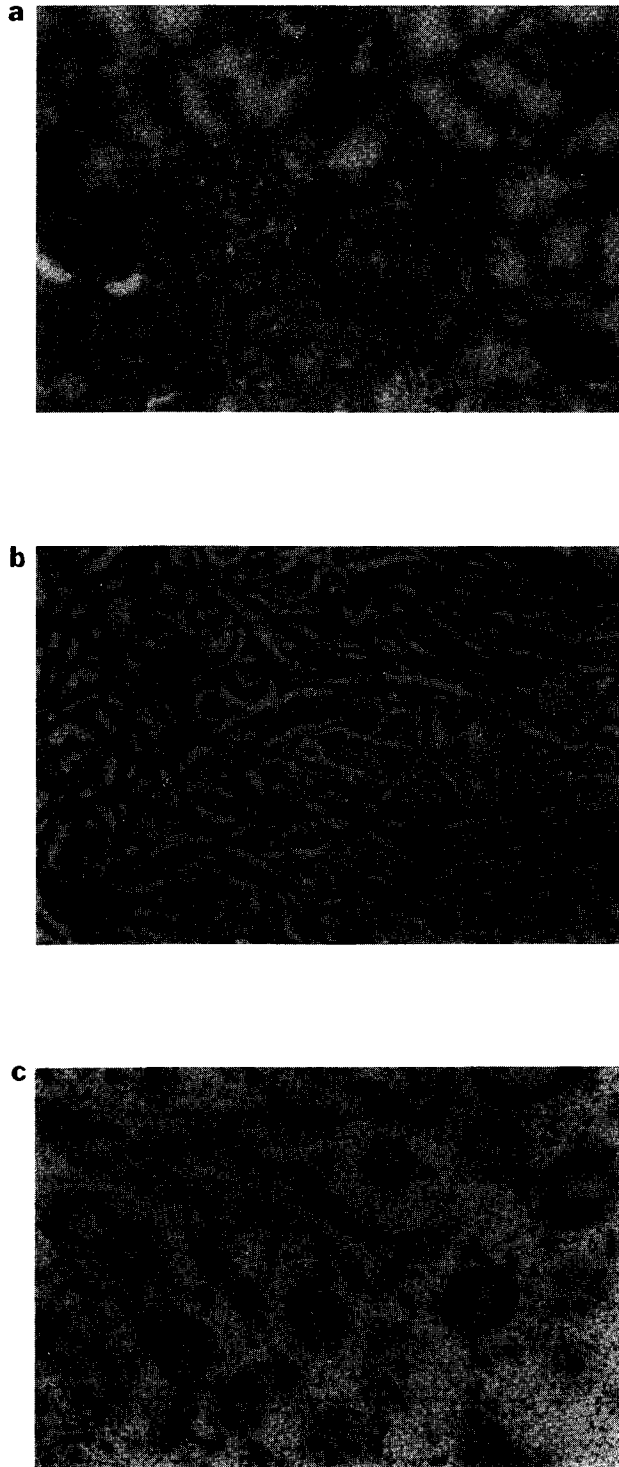


Fig. 4. Morphologic demonstration of intrarenal distribution of  $^{125}\text{I}$ -radioactivity determined by autoradiography after the i.v. administration of  $^{125}\text{I}$ -EGF ( $10\ \mu\text{Ci}/\text{rat}$ ). The silver grains were observed to be high on the luminal side of the PCT (1) and the antiluminal side of the PT (2) but to be lower in the CT (3) and glomeruli (4). (a) Cortex; (b and c) outer medulla and inner medulla, respectively. In the inner medulla, the silver grains were observed in the CD (1) and TLH (2).

(6) based on binding assays of EGF in those isolated nephron segments or based on the observation of the physiological effects induced by EGF. We previously investigated the renal handling of EGF in the nonfiltering perfused rat kidney, where the EGF receptor is accessible only from the antiluminal side (15). We investigated also the distribution of antiluminal EGF binding sites along the nephron in the nonfiltering kidney by autoradiography (20). We found (i) the presence of high-affinity binding sites ( $K_{d1} = 0.1\ \text{nM}$ ,  $K_{d2} = 30\ \text{nM}$ ) and receptor-mediated endocytosis (RME) via the antiluminal membrane after the binding of EGF to those high-affinity sites (15) and (ii) that the EGF-binding sites were distributed over the entire kidney, and  $^{125}\text{I}$ -EGF binding was high in the proximal straight tubule (PST), inner medullary thin limb of Henle (IMTLH), and IMCD (20).

To detect EGF binding sites on the luminal cell surface membrane, a recirculatory perfusion of  $^{125}\text{I}$ -EGF was performed in the filtering kidney. The  $^{125}\text{I}$  radioactivity which appeared in the outflow from the urinary cannula by acid washing could have been released from  $^{125}\text{I}$ -EGF bound to the luminal cell surface membrane, mesangial cells, or glomerular capillaries. In fact, EGF receptors have been identified in cultured mesangial cells (4). However, cortical  $^{125}\text{I}$  radioactivity was observed mainly in the proximal convoluted tubule (PCT), not in glomeruli (Table IV). Further,  $^{125}\text{I}$  radioactivity was high on the luminal cell surface membrane of PCT after i.v.  $^{125}\text{I}$ -EGF administration, and exposed silver grains moved from the luminal cell surface to the intracellular space (Table IV). These results suggest that the  $^{125}\text{I}$  radioactivity eluted from the urinary cannula by acid washing comes from the bound  $^{125}\text{I}$ -EGF on the luminal cell surface membrane of PCT. These  $^{125}\text{I}$ -EGF binding sites are thought to be of a low affinity compared to those on the antiluminal cell surface membrane, since the amount of luminal cell surface bound  $^{125}\text{I}$ -EGF [ $\text{LR}_s(\text{LM})$ ] was not changed in the presence of  $20\ \text{nM}$  unlabeled EGF (Table I). Therefore, the remarkable reduction of internalized EGF ( $\text{LR}_i$ ) in the presence of excess unlabeled EGF is due to the saturation of EGF binding to the antiluminal cell surface membrane receptor. Our previous kinetic analysis using nonfiltering and filtering isolated perfused rat kidneys predicted these results (15).

The assumption that the reabsorption of EGF through the luminal membrane took place mainly in the cortex and outer medulla was suggested from the tissue sampling study (Table III) and comparison of  $^{125}\text{I}$ -EGF distribution as determined by autoradiography in the *in vivo* and nonfiltering kidneys. *In vivo* autoradiography showed the highest  $^{125}\text{I}$ -EGF binding in the cortex (Table II, Fig. 2). On the other hand,  $^{125}\text{I}$ -EGF binding was shown to be high in the inner medullary, followed by the cortex and outer medulla, by previous autoradiographic studies in the nonfiltering kidney (20). In the nonfiltering kidney, glomerular filtration is negligible, resulting in different results between the *in vivo* and the nonfiltering kidneys. Thus, a high abundance of the cortex and outer medulla binding sites available to filtered EGF can account for the observed difference. The present experiment using filtering perfused kidney indicated the binding of  $^{125}\text{I}$ -EGF to the antiluminal cell surface membrane [ $\text{LR}_s(\text{ALM})$ ] was remarkably inhibited by the addition of

Table IV. Localization of Binding Sites for  $^{125}\text{I}$ -EGF<sup>a</sup>

Time (min)	COR					
	PT		Glo	CT	IM	
	SI(PCT)	(S2 + S3)			TLH	CD
2 (N = 3)						
Whole	ND	ND	0.14 ± 0.04	0.15 ± 0.09	0.21 ± 0.07	0.04 ± 0.01
ALM	0.46 ± 0.13	0.86 ± 0.13	ND	ND	ND	ND
Cell	1.35 ± 0.41	0.10 ± 0.06	ND	ND	ND	ND
LM	4.21 ± 0.66	0.01 ± 0.01	ND	ND	ND	ND
10 (N = 2)						
Whole	ND	ND	0.19	0.09	0.28	0.11
ALM	0.29	1.40	ND	ND	ND	ND
Cell	2.71	0.82	ND	ND	ND	ND
LM	1.98	0.28	ND	ND	ND	ND

<sup>a</sup> Grain number per unit area was determined. After the i.v. injection of  $^{125}\text{I}$ -EGF (10  $\mu\text{Ci}/\text{rat}$ ), the kidney was fixed with 2% glutaraldehyde in saline. To observe the binding sites of  $^{125}\text{I}$ -EGF histologically, the paraffin sections (4  $\mu\text{m}$  thick) were mounted on glass slides. After the preparations were developed and fixed, they were stained with hematoxylin-eosin. The silver grains were counted with the use of an image analyzer (IBAS, Carl Zeiss, Germany). COR, cortex; IM, inner medulla; PT, proximal tubule; Glo, glomerulus; CT, collecting tubule; TLH, thin limb of Henle; CD, collecting duct; SI(PCT), proximal convoluted tubule; S2 + S3, proximal tubule except the S1 segment; ALM, antiluminal membrane; LM, luminal membrane; Cell, intracellular space; ND, not determined.

excess unlabeled EGF (20 nM) to the perfusate, but that to the luminal cell surface membrane [LR<sub>s</sub>(LM)] was not inhibited (Table I). Thus, the saturability of EGF binding differs in each kidney fraction: (i) In the inner medulla, the high-affinity binding sites of EGF are mainly on the antiluminal cell surface membrane; and (ii) in addition to the antiluminal high-affinity sites, the low-affinity sites of EGF on the luminal cell surface membrane were also abundant in the cortex and outer medulla. Besides the function as clearance receptor which controls the plasma levels of EGF, the EGF receptor on the antiluminal membrane of the kidney may play an important role in the control of renal physiology. An EGF infusion (1.25  $\mu\text{g}/\text{hr}$  i.v. for 6 hr) in sheep showed an increase in urine flow and urinary Na<sup>+</sup> and K<sup>+</sup> excretion (24). The application of EGF (17 pM–17 nM) to the antiluminal side of the cortical collecting tubule isolated from rabbit decreased sodium reabsorption by 44–59% (25). Therefore, it is likely that these pharmacologic effects are induced via the EGF binding by the antiluminal membrane receptor.

We then identified the binding sites histologically (Fig. 4). The exposed silver grains moved from the luminal cell surface membrane to the intracellular space in the PCT with time (Table IV), suggesting the internalization of filtered EGF via luminal cell surface membrane. On the other hand, in the PT (S2 + S3), the exposed silver grain density ratios of antiluminal cell surface membrane to the intracellular space decreased with time (Table IV), suggesting the internalization of  $^{125}\text{I}$ -EGF from the antiluminal side, as observed previously using the nonfiltering perfused rat kidney (20).

EGF binding sites were thus identified on the luminal cell surface membrane of the PCT. EGF binding to brush border membranes isolated from rat or rabbit kidneys was previously observed (26,27). However, the much lower specific binding compared with that to basolateral membrane may be accounted for by cross-contamination of the brush

border with basolateral membranes (26,27). Recently, Nielsen *et al.* (28) exposed isolated and perfused rabbit proximal tubules to  $^{125}\text{I}$ -EGF either in the perfusate or in the bath fluid. Although the fractional transtubular transport of  $^{125}\text{I}$ -EGF from the perfusate (lumen) to the bath (basolateral side) was small, it was significant and much higher than that of inulin. This result (28) is consistent with the significant uptake of  $^{125}\text{I}$ -EGF from the luminal membrane of renal proximal tubules. Further, uptake (internalization) occurred after  $^{125}\text{I}$ -EGF binding to the luminal membrane of PCT in the cortex and probably in the outer medulla (Tables III and IV, Fig. 4). However, it remains unclear whether the low-affinity binding sites in these regions were bonafide EGF receptors.

Breyer *et al.* (29) determined the relative density of EGF receptors using microdissected nephron segments isolated from rabbit kidney. Specific  $^{125}\text{I}$ -EGF binding was highest in proximal straight tubules (PST), followed by PCT, collecting ducts in cortical, inner medullar and outer medulla regions, and distal tubules; however, they did not discriminate whether the EGF binding sites were localized on the antiluminal membrane or on the luminal membrane.

Figure 5 represents the intrarenal distribution of EGF binding sites, on the basis of the present study. The localization of prepro-EGF mRNA (5) is also shown. The EGF binding sites on the luminal cell surface membrane of the PCT seem to be inaccessible to endogenous EGF, which was synthesized and excreted to the lumen of TALH or DCT, located in a more distal part of the nephron than the PCT (5). Considering that the PCT is the earliest site with which the filtered EGF had contact, the reabsorption mechanism of filtered EGF in the PCT may control the delivery of filtered EGF to the more distal part of nephron. The origin of urinary EGF is controversial. Because urinary EGF levels parallel those of urine creatinine in humans, it would appear that the kidney simply filters EGF in the glomeruli (19,30).

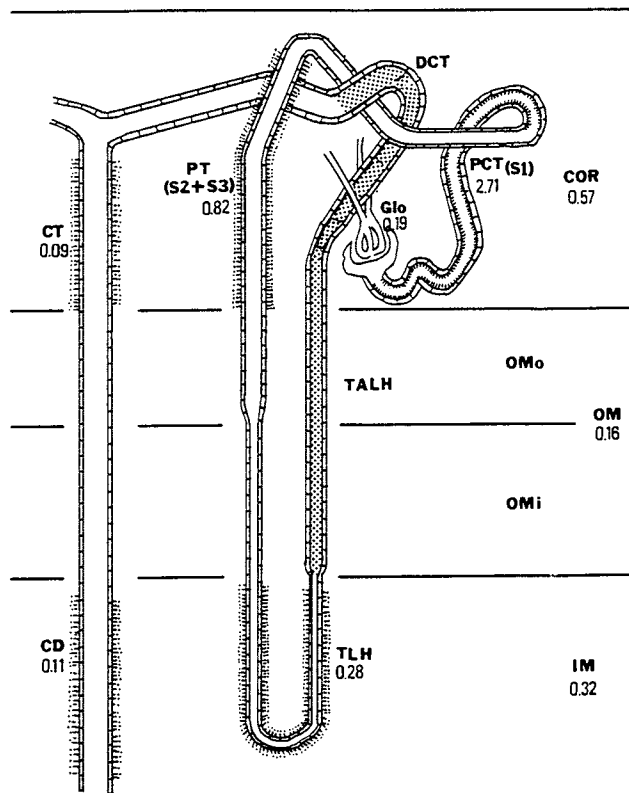


Fig. 5. Schematic representation of the intrarenal distribution of EGF binding sites and prepro-EGF mRNA along the nephron. COR, cortex; OM, outer medulla; OMo, outer stripe of outer medulla; OMi, inner stripe of outer medulla; IM, inner medulla; PCT(S1), proximal convoluted tubule; Glo, glomeruli; PT(S2 + S3), proximal tubule; TLH, thin limb of Henle; CT, cortical collecting tubule; CD, inner medullary collecting duct; TALH, thick ascending limb of Henle; DCT, distal convoluted tubule. ( ▨ ) The distribution of prepro-EGF mRNA in TALH and DCT, reported previously (5). ( ▨ ) Antiluminal binding sites of  $^{125}\text{I}$ -EGF on the CD, CT, TLH, and PT(S2 + S3). ( ▨ ) Luminal binding sites of  $^{125}\text{I}$ -EGF on the PCT(S1). Numbers show the relative density of  $^{125}\text{I}$ -EGF binding obtained from the kidney 10 min after the i.v. administration of tracer  $^{125}\text{I}$ -EGF (10  $\mu\text{Ci}/\text{rat}$ ). The numbers for PCT, Glo, PT, CT, TLH, and CD are obtained from Table IV, while the numbers for COR, OM, and IM are obtained from Table II.

However, several observations in rat and mice indicate that EGF synthesized in the kidney and/or EGF in the circulating plasma is secreted to the lumen (31,32). In either case, some of the urinary EGF comes from filtration through glomeruli, and the reabsorption mechanism may play a role in the control of the amount of EGF excreted in the urine.

In conclusion, the reabsorption mechanism of filtered EGF through low-affinity binding sites on the luminal cell surface membrane was demonstrated.

## REFERENCES

1. S. Cohen and G. Carpenter. Human epidermal growth factor: Isolation and chemical and biological properties. *Proc. Natl. Acad. Sci. USA* 72:1317-1321 (1975).
2. P. R. Goodyer, E. Kachra, C. Bell, and R. Rozen. Renal tubular cells are potential targets for epidermal growth factor. *Am. J. Physiol.* 255 (Renal Fluid Electrolyte Physiol. 24):F1191-F1196 (1988).
3. Y. Hirata and D. N. Orth. Epidermal growth factor (urogastrone) in human fluids: Size heterogeneity. *J. Clin. Endocrinol. Metab.* 48:673 (1979).
4. H. Gregory. Isolation and structure of urogastrone and its relation to epidermal growth factor. *Nature* 257:104-108 (1975).
5. L. B. Rall, S. James, I. B. Graeme, J. C. Robert, D. P. Jennifer, D. N. Hugh, and P. C. John. Mouse prepro-epidermal growth factor synthesis by the kidney and other tissues. *Nature* 314:228-231 (1985).
6. D. Fisher, E. Salido, and L. Barajas. Epidermal growth factor and the kidney. *Annu. Rev. Physiol.* 51:67-80 (1989).
7. R. C. Harris, R. L. Hoover, H. R. Jacobson, and K. F. Badr. Evidence for glomerular actions of epidermal growth factor in the rat. *J. Clin. Invest.* 82:1028-1039 (1988).
8. J. Norman, B. Badie-Dezfooly, E. P. Nord, I. Kurtz, J. Schlosser, A. Chaudhari, and L. G. Fine. EGF-induced mitogenesis in proximal tubular cells: Potentiation by angiotensin II. *Am. J. Physiol.* 253 (Renal Fluid Electrolyte Physiol. 22):F299-F309 (1987).
9. V. M. Vehaskari, K. S. Hering-Smith, D. W. Moskowitz, I. D. Weiner, and L. L. Hamm. Effect of epidermal growth factor on sodium transport in the cortical collecting tubule. *Am. J. Physiol.* 256 (Renal Fluid Electrolyte Physiol. 25):F803-F809 (1989).
10. D. C. Kim, Y. Sugiyama, H. Sato, T. Fuwa, T. Iga, and M. Hanano. Kinetic analysis of *in vivo* receptor dependent binding of human epidermal growth factor by rat tissues. *J. Pharm. Sci.* 77:200-207 (1988).
11. D. C. Kim, Y. Sugiyama, T. Fuwa, S. Sakamoto, T. Iga, and M. Hanano. Kinetic analysis of the elimination process of human epidermal growth factor in rats. *Biochem. Pharmacol.* 38:241-249 (1989).
12. Y. Sugiyama, D. C. Kim, H. Sato, S. Yanai, H. Satoh, T. Iga, and M. Hanano. Receptor-mediated disposition of polypeptides: Kinetic analysis of the transport of epidermal growth factor as a model peptide using *in vitro* isolated perfused organs and *in vivo* system. *J. Control. Release* 13:157-174 (1990).
13. Y. Sugiyama and M. Hanano. Receptor-mediated transport of peptide hormones and its importance in the overall hormone disposition in the body. *Pharm. Res.* 6:192-202 (1989).
14. D. C. Kim, Y. Sugiyama, Y. Sawada, and M. Hanano. Renal tubular handling of p-aminohippurate and epidermal growth factor in the filtering and nonfiltering perfused rat kidneys. *Pharm. Res.* 9:271-275 (1992).
15. D. C. Kim, M. Hanano, T. Iga, and Y. Sugiyama. Kinetic analysis of receptor-mediated endocytosis of epidermal growth factor in isolated perfused rat kidney. *Am. J. Physiol.* 261 (Renal Fluid Electrolyte Physiol. 30):F988-F997 (1991).
16. T. Oka, S. Sakamoto, K. I. Miyoshi, T. Fuwa, K. Yoda, M. Yamasaki, G. Tamura, and T. Miyake. Synthesis and secretion of human epidermal growth factor by *Escherichia coli*. *Proc. Natl. Acad. Sci. USA* 82:7212-7216 (1985).
17. I. Vlodavsky, D. B. Kenneth, and G. Denis. A comparison of the binding of epidermal growth factor to cultured granulosa and luteal cells. *J. Biol. Chem.* 253:3744-3750 (1978).
18. N. Ito, Y. Sawada, Y. Sugiyama, T. Iga, and M. Hanano. Kinetic analysis of rat renal tubular transport based on multiple indicator dilution method. *Am. J. Physiol.* 251 (Renal Fluid Electrolyte Physiol. 20):F103-F114 (1986).
19. F. H. Epstein, J. T. Brosnan, J. D. Tange, and B. D. Ross. Improved function with amino acids in the isolated perfused kidney. *Am. J. Physiol.* 243 (Renal Fluid Electrolyte Physiol. 12):F284-F292 (1982).
20. D. C. Kim, Y. Sugiyama, Y. Kanai, N. Ohnuma, and M. Hanano. Localization of EGF binding sites on antiluminal plasma membrane of rat kidney: Autoradiographic study using nonfiltering perfused rat kidney. *Pharm. Res.* 9:40-44 (1992).
21. S. T. Kan and T. Maack. Transport and catabolism of parathyroid hormone in isolated rat kidney. *Am. J. Physiol.* 233 (Renal Fluid Electrolyte Physiol. 2):F445-F454 (1977).
22. J. J. M. Bergeron, R. Rachubinski, N. Searle, D. Borts, R. Sikstrom, and B. I. Posner. Polypeptide hormone receptors *in vivo*: Demonstration of insulin binding to adrenal gland and

- gastrointestinal epithelium by quantitative radioautography. *J. Histochem. Cytochem.* 28:824-835 (1980).
23. R. C. Harris. Response of rat inner medullary collecting duct to epidermal growth factor. *Am. J. Physiol.* 256 (*Renal Fluid Electrolyte Physiol.* 25):F1117-F1124 (1989).
  24. B. A. Scoggins, A. Butkus, J. P. Coghlan, D. T. W. Fei, I. G. McDougall, H. D. Niall, J. R. Walsh, and X. Wang. *In Vivo Cardiovascular Renal and Endocrine Effects of Epidermal Growth Factor in Sheep*, Elsevier, New York, 1984, pp. 573-575.
  25. V. M. Vehaskari, K. S. Hering-Smith, D. W. Moskowitz, I. D. Weiner, and L. L. Hamm. Effect of epidermal growth factor on sodium transport in the cortical collecting tubule. *Am. J. Physiol.* 256 (*Renal Fluid Electrolyte Physiol.* 25):F803-F809 (1989).
  26. R. C. Harris and T. O. Daniel. Epidermal growth factor binding, stimulation of phosphorylation, and inhibition of gluconeogenesis in rat proximal tubule. *J. Cell. Physiol.* 139:383-391 (1989).
  27. E. Sack and Z. Talor. High affinity binding sites for epidermal growth factor (EGF) in renal membranes. *Biochem. Biophys. Res. Commun.* 154:312-317 (1988).
  28. S. Nielsen, E. Nexø, and E. I. Christensen. Absorption of epidermal growth factor and insulin in rabbit renal proximal tubules. *Am. J. Physiol.* 256 (*Endocrinol. Metab.* 19):E55-E63 (1989).
  29. M. D. Breyer, R. Redha, and J. A. Breyer. Segmental distribution of epidermal growth factor binding sites in rabbit nephron. *Am. J. Physiol.* 25X (*Renal Fluid Electrolyte Physiol.* 28):F553-F558 (1990).
  30. R. H. Starkey and D. N. Orth. Radioimmunoassay of human epidermal growth factor (urogastrone). *J. Clin. Endocrinol. Metab.* 45:1144-1153 (1977).
  31. R. S. Olsen, E. Nexø, S. S. Poulsen, H. F. Hansen, and P. K. Kirkegaard. Renal origin of rat urinary epidermal growth factor. *Regul. Pept.* 10:37-45 (1984).
  32. J. Perheentupa, J. Lakshmanan, S. B. Hoath, and D. A. Fisher. Epidermal growth factor in mouse urine: Non-blood origin and increase by sialoadenectomy and T<sub>4</sub> therapy. *Acta Endocrinol.* 108:428-432 (1985).